fibers

MDPI

Article

Ultrashort Pulse Retrieval from Experimental Spectra Transformed in Chalcogenide and Silica Fibers

Elena A. Anashkina *, Arseny A. Sorokin and Alexey V. Andrianov

Institute of Applied Physics of the Russian Academy of Sciences, 46 Ulyanov Street, Nizhny Novgorod 603950, Russia
* Correspondence: elena.anashkina@ipfran.ru

Abstract: The characterization of ultrashort optical pulses is a highly requested task. The most popular commercially available hardware/software systems are based on interferometric measurements and second-harmonic generation, leading to some ambiguities and limitations. Here we experimentally test the non-interferometric method of pulse retrieval from three spectra: the fundamental spectrum and two spectra that transformed in an element with Kerr nonlinearity and accumulated different nonlinear phases (different *B*-integrals). This method has no ambiguities related to time direction, and allows simple hardware/software implementation. We test a novel simple algorithm for experimental data processing based on the search for a polynomial-approximated spectral phase. Two experimental cases are considered. In the first one, we retrieved 160 fs pulses using a chalcogenide arsenic sulfide glass fiber as a nonlinear Kerr element. In the second case, we retrieved 670 fs pulses with a complex spectrum using a piece of silica-based fiber. The results are confirmed by independent measurements using a standard SHG-FROG technique (Second-Harmonic Generation Frequency-Resolved Optical Gating).

Keywords: chalcogenide fibers; Kerr nonlinearity; pulse retrieval; spectral phase retrieval

check for updates

Citation: Anashkina, E.A.; Sorokin, A.A.; Andrianov, A.V. Ultrashort Pulse Retrieval from Experimental Spectra Transformed in Chalcogenide and Silica Fibers. *Fibers* **2022**, *10*, 98. https://doi.org/10.3390/fib10110098

Academic Editor: Walter Belardi

Received: 11 October 2022
Accepted: 8 November 2022
Published: 11 November 2022

Publisher's Note: MDPI stays neutral with regard to jurisdictional claims in published maps and institutional affiliations.

Copyright: © 2022 by the authors. Licensee MDPI, Basel, Switzerland. This article is an open access article distributed under the terms and conditions of the Creative Commons Attribution (CC BY) license (https://creativecommons.org/licenses/by/4.0/).

1. Introduction

The characterization of ultrashort optical pulses is in demand for solving many problems. The most popular commercially available hardware/software systems, such as autocorrelators and Second-Harmonic Generation Frequency-Resolved Optical Gating (SHG-FROG) are based on interferometric measurements and second-harmonic generation, leading to some ambiguities and limitations [1,2]. The ambiguities concern the direction of the temporal axis and the sign of the phase; the main limitations concern the spectral width, since nonlinear crystals have limited phase-matching bandwidths. To date, there are a lot of different methods, and their modifications for ultrashort pulse characterization have various degrees of complexity, advantages, and shortcomings [2–8]. Nevertheless, the development of ultrafast metrology with simple hardware/software implementations and without ambiguities is in demand.

A simple non-interferometric method using 3rd-order Kerr nonlinearity rather than 2nd-order nonlinearity was proposed in [9]. It is based on measuring the fundamental (non-transformed) pulse spectrum and two self-phase modulated (SPM) spectra with different values of *B*-integrals [9]. The iterative Gerchberg–Saxton-like numerical algorithm was developed for data processing [9]. This method was successfully implemented to characterize high-power single-shot pulses using thin plastic films as nonlinear Kerr elements [9], and for pulses with less power in the telecommunication range using optical fibers as nonlinear elements [10–13]. It should be emphasized that in previous papers [9–13], various iterative Gerchberg–Saxton-like numerical algorithms were used for spectra processing. However, such numerical algorithms work well for pulses with a relatively small phase (not more than π). For strongly chirped pulses, it may be challenging to find the global, rather than

local, minimum of an error function. Very recently, to overcome this challenge, we proposed a novel simple and fast algorithm for processing the fundamental spectrum together with two SPM spectra with different values of *B*-integrals [14]. The algorithm is based on searching for the polynomial-approximated spectral phase minimizing the error function, which is the difference between the measured and retrieved SPM spectra [14]. An exhaustive search is run to find optimal polynomial coefficients. Additionally, we numerically showed that this approach can be applied to characterize mid-IR ultrashort pulses using commercial chalcogenide glass fibers [14]. Here we demonstrate experimental implementations of the method using the novel algorithm of searching for a polynomial-approximated spectral phase. As far as we know, this is the first experimental verification of the algorithm on measured (not numerically simulated) data. In particular, we report the pulse retrieval using a nonlinear silica-based fiber and a chalcogenide (arsenic-sulfide-based) fiber. The use of a chalcogenide fiber as a nonlinear element in this method is also demonstrated for the first time. This successful experiment with a chalcogenide fiber in the telecommunication range motivates further studies on pulse retrieval in the wavelength range well beyond 2 μm, where the use of chalcogenide fibers is more justified since silica fibers are not transparent. The obtained results are verified by independent standard SHG-FROG measurements.

2. Methods

2.1. Numerical Algorithm

The tested method for ultrashort pulse retrieval is based on measuring and processing three spectra: fundamental spectrum $I_0(f)$ (hereinafter f is frequency) and two SPM spectra transformed in a nonlinear fiber. The SPM spectra $I_1(f)$ and $I_2(f)$ correspond to different B_1 and B_2 values of *B*-integrals ($B = \int_0^L \gamma P(z)dz$, where γ is the nonlinear coefficient, P is pulse peak power, z is the longitudinal coordinate, and L is fiber length). The main idea of the method and the block diagram of the tested algorithm are presented in Figure 1a,b, respectively. The details can be found in [14]. In brief, the algorithm finds an optimal polynomial-approximated spectral phase ${\varphi_0}^{\text{opt}}$ minimizing the difference between measured and retrieved SPM spectra [14]. An exhaustive search for polynomial coefficients is run on a reasonable grid [14].

The evolution of the complex field amplitude $E(t, z)$ (neglecting dispersion) in a nonlinear fiber is given by [15]

$$\frac{\partial E(t,z)}{\partial z} = i\gamma |E(t,z)|^2 E(t,z) \tag{1}$$

The field envelopes $E_1(t)$ and $E_2(t)$ of the output pulses after propagation in the fiber are

$$E_1(t) = E_0(t) \exp\left(iB_1 |E_0(t)|_2 / \max(|E_0(t)|_2) \right), \tag{2}$$

$$E_2(t) = E_0(t) \exp\left(iB_2 |E_0(t)|_2 / \max(|E_0(t)|_2) \right), \tag{3}$$

where $E_0(t)$ is the complex field envelope of the input pulse. The dispersionless approximation is reasonable when the dispersion length L_D is much longer than L ($L_D = \tau^2 / |\beta_2| >> L$, where τ is the pulse duration and β_2 is the second-order dispersion coefficient [15]).

The spectral complex amplitudes are defined as

$$\widetilde{E}_{0,1,2}(f) = \hat{F}[E_{0,1,2}(t)], \tag{4}$$

where $\hat{F}$ is the Fourier transform operator. Assuming that φ_0 is the guessed spectral phase of the characterized pulse, we can write

$$E_0(t) = \hat{F}^{-1}\left[\widetilde{E}_0(f)\right] = \hat{F}^{-1}\left[\sqrt{I_0(f)}\exp(i\varphi_0)\right]. \tag{5}$$

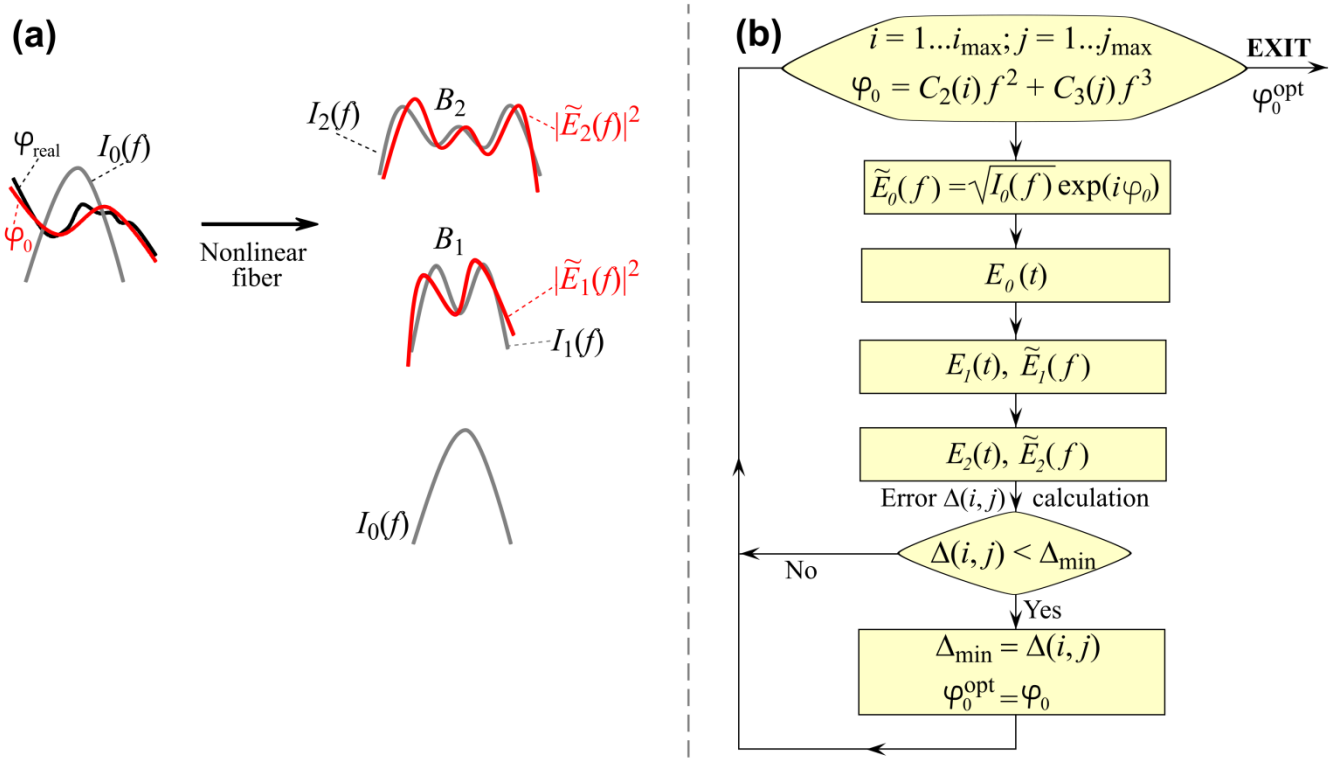

Figure 1. (**a**) Schematic representation of the method for pulse retrieval from fundamental and two SPM spectra transformed in the nonlinear fiber. (**b**) Block diagram of the tested algorithm for optimizing polynomial-approximated spectral phase (for preset *B*-integrals).

Next, we can calculate $E_1(t)$ and $E_2(t)$ using Formulas (2) and (3). $\left|\tilde{E}_1(f)\right|^2$ and $\left|\tilde{E}_2(f)\right|^2$ are close to $I_1(f)$ and $I_2(f)$, respectively, if φ_0 is close to the real spectral phase φ_{real} (Figure 1a) [9,14]. To quantitatively describe the similarity of the real and retrieved SPM spectra, we use the following error function

$$\Delta = \frac{1}{2} \frac{\left[\sum_{k=1}^{N} \left(\left|\tilde{E}_1(f_k)\right|^2 - I_1(f_k) \right)^2 + \sum_{k=1}^{N} \left(\left|\tilde{E}_2(f_k)\right|^2 - I_2(f_k) \right)^2 \right]^{1/2}}{\sum_{k=1}^{N} I_0(f_k)}, \quad (6)$$

where N is the number of the chosen frequency points and f_k is the frequency at the k-th point.

We assume that the spectral phase can be approximated by a cubic polynomial with sufficient accuracy; $\varphi_0(f) = C_2 f^2 + C_3 f^3$. We minimize the error function using an exhaustive search for C_2 and C_3 (Figure 1b) [14]. The values of $C_2{}^{(0)}$ and $C_3{}^{(0)}$ correspond to the global minimum of Δ; $\varphi_0^{opt}(f) = C_2^{(0)} f^2 + C_3^{(0)} f^3$.

As a rule, *B*-integrals are not exactly known but their ratio B_2/B_1 is known. Therefore, the algorithm is run for various B_2 and after that the value minimizing Δ is selected [14]. Note that the ratio of *B*-integrals should not be very close to 1. Otherwise, the SPM spectra are very similar, which may lead to errors in their processing, especially with allowance for noise. We set B_2/B_1 as ≥ 1.5.

2.2. Experimental Schemes

For experimental testing of the algorithm optimizing the polynomial-approximated spectral phase, we used two setups based on a femtosecond Er-doped fiber laser. The schemes are shown in Figure 2a,b. In both cases, the systems start from the Er-doped fiber

master oscillator with passive mode locking using a nonlinear polarization rotation. The laser generates ultrashort pulses at a central wavelength of 1.56 μm with a repetition rate of 50 MHz.

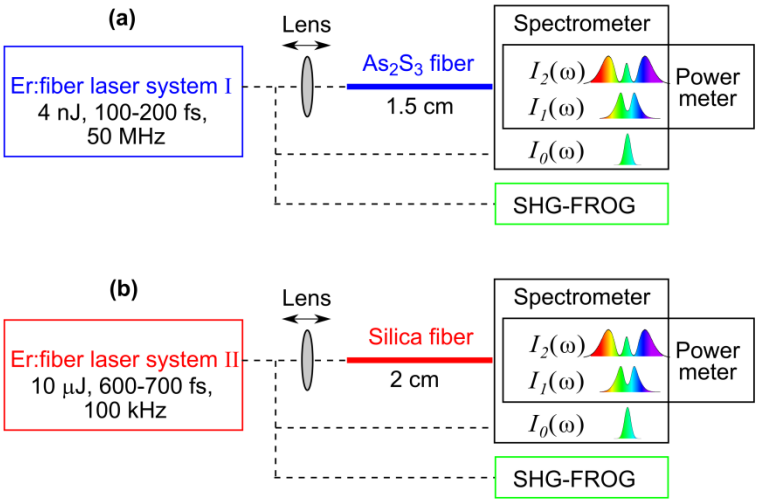

Figure 2. Simplified experimental schemes for pulse measurements using a chalcogenide fiber (**a**) and a silica fiber (**b**) as nonlinear elements.

In the first investigated case, "Er:fiber laser system I" contains a single-fiber amplifier. The maximum output pulse energy is 4 nJ. The phase is not flat due to the nonlinear and dispersive effects in the amplifier. This system is similar to the one reported in [16]. Here, a chalcogenide As_2S_3 glass fiber is used as a nonlinear Kerr element. Laser pulses from the output of "Er:fiber laser system I" are coupled to 1.5 cm As_2S_3 fiber through a lens (Figure 2a). The coupling efficiency is regulated by tuning the lens focus relative to the chalcogenide fiber input. This allows us to control the ratio of *B*-integrals by monitoring average output powers (B_2/B_1 is proportional to the ratio of average powers). The coupling efficiency was of the order of a few percent. The standard SHG-FROG technique was used to independently measure the tested pulses (Figure 2a).

In the second case, we characterized the pulses from the output of "Er: fiber laser system II" delivering maximum energy of about 10 μJ (although this value was attenuated down to ~1 μJ). The system configuration is similar to that reported in [17]. This system operates in a chirped pulse amplification regime. A fiber stretcher is used after the master oscillator before two fiber preamplifiers and the final amplifying cascade. The pulse repetition rate is decreased from 50 MHz to 100 kHz by an acousto-optic modulator inserted between two preamplifiers. This is conducted to reduce the average power. The pulses at the output of the final fiber amplifying cascade pass through a grating compressor and after that are propagated in a short piece of a standard telecommunication fiber (of order 1 cm) to broaden the spectrum and to accumulate an additional phase due to SPM. This is conducted to test the applicability of the method for retrieving the additional phase. Furthermore, as in the previous scheme, the pulses are coupled through the lens into a segment of a nonlinear fiber playing a key role in the tested method (Figure 2b). In this experiment, we used a silica-based fiber with a smaller diameter compared to SMF28e and with a larger nonlinear Kerr coefficient due to a smaller mode field area. The SHG-FROG technique was also used to verify the results obtained with the tested method.

3. Results

3.1. Pulse Retrieval from Measurements Using Chalcogenide Fiber

In the first experiment, we used the scheme presented in Figure 2a. We took a small piece of a chalcogenide fiber, 1.5 cm long, as an element for spectrum transformation due to SPM. Here, the estimated dispersion length of the order of 10 cm is much longer than the fiber length ($L >> L_D$), thus the dispersionless approximation is reasonable. For this fiber,

the calculated nonlinear Kerr coefficient is γ~300 (W km)$^{-1}$. We measured the fundamental and two transformed SPM spectra, and after that applying the described algorithm for finding the polynomial-approximated spectral phase, we retrieved the temporal intensity profile (Figure 3a) and the temporal phase (Figure 3b). The error function is visualized in Figure 3c. In this case, the optimal polynomial coefficients minimizing the error are $C_2^{(0)} = 0.044$ ps^2 and $C_3^{(0)} = -0.001$ ps^3. The fundamental spectrum of the signal is shown in Figure 3d. The SPM measured and retrieved spectra are plotted in Figure 3e,f for two different values of the B-integrals: $B_1 = 0.8$ and $B_2 = 1.3$. The pulse duration is 160 fs (full width at half maximum, FWHM), which is in excellent agreement with the results of independent SHG-FROG measurements also shown in Figure 3a. The temporal phases retrieved using the tested method and SHG-FROG also coincide almost perfectly (Figure 3b). It should be noted that the SHG-FROG method exhibits ambiguity in the choice of the direction of the time axis and the phase sign. To eliminate this ambiguity, we took into account the results of our method, which produced an unambiguous answer. Note that the execution time of the tested algorithm for processing experimental spectra was only a few seconds (to calculate the whole error map in Figure 3c).

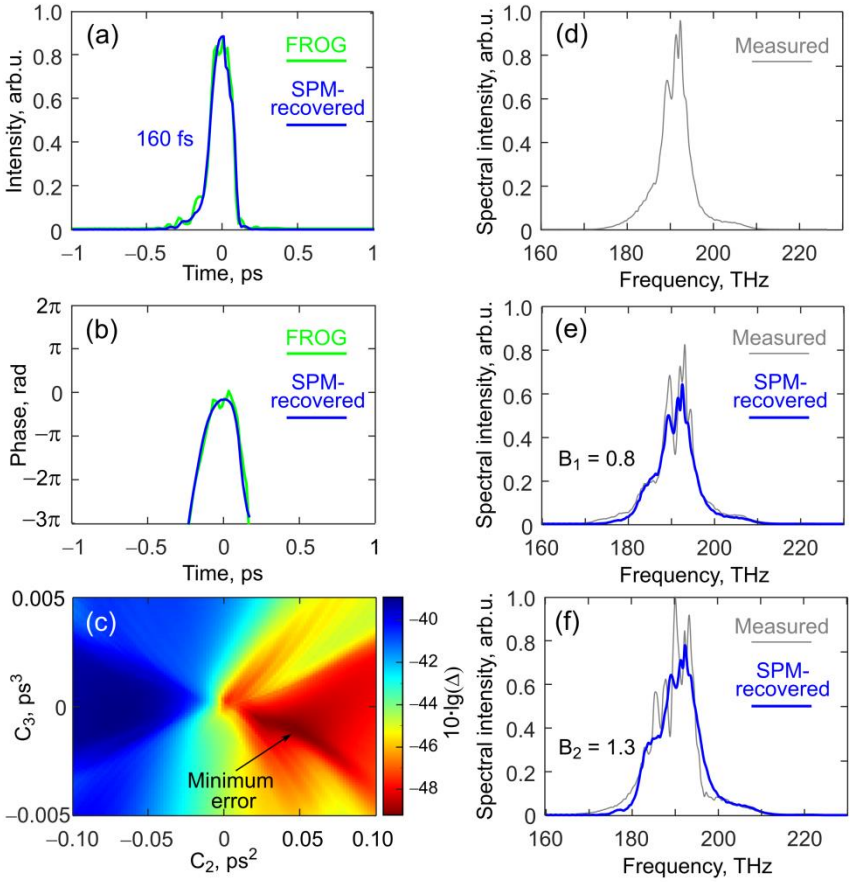

Figure 3. Pulse retrieval from measurements using a ***chalcogenide fiber***. Retrieved temporal intensity distribution (**a**) and temporal phase (**b**) using the tested approach (blue curves) and independent SHG-FROG technique (green curves). (**c**) Calculated function 10·lg(Δ). (**d**) Measured fundamental spectrum. Measured and retrieved SPM spectra for $B_1 = 0.8$ (**e**) and $B_2 = 1.3$ (**f**).

3.2. Pulse Retrieval from Measurements Using a Silica Fiber

In the second experiment, we used the scheme sketched in Figure 2b. A 2 cm silica-based fiber was chosen as a nonlinear Kerr element. Its nonlinear Kerr coefficient is γ~4 (W km)$^{-1}$. As in the first experiment, here we also measured the fundamental and two transformed SPM spectra, and after that, we applied the tested algorithm for finding the polynomial-approximated spectral phase. In contrast to the previous case, when the B-integrals were

of order 1, here the *B*-integrals were large (of order 10) and the transformed spectra were significantly broadened and strongly modulated. We found that the tested algorithm works correctly in this case as well. The retrieved temporal intensity profile and temporal phase are shown in Figure 4a,b, respectively. The error function is demonstrated in Figure 4c. The optimal polynomial coefficients are $C_2^{(0)} = 1.3$ ps^2 and $C_3^{(0)} = -0.015$ ps^3. The fundamental spectrum and two SPM spectra with $B_1 = 6.5$ and $B_2 = 11$ are presented in Figure 4d–f, respectively. The obtained pulse with a FWHM duration of 670 fs agrees sufficiently well with the SHG-FROG pulse (Figure 4a). The temporal phases retrieved from the tested method and the SHG-FROG are also close to each other (Figure 4b).

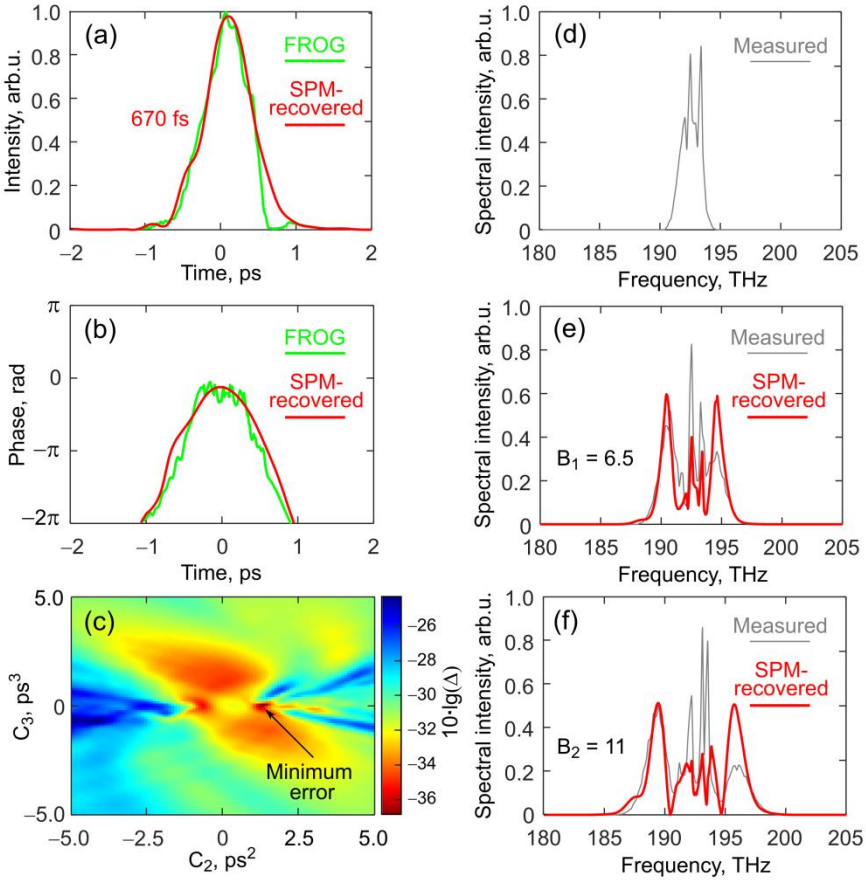

Figure 4. Pulse retrieval from measurements using a ***silica fiber***. Retrieved temporal intensity distribution (**a**) and temporal phase (**b**) using the tested approach (blue curves) and independent SHG-FROG technique (green curves). (**c**) Calculated function 10·lg(Δ). (**d**) Measured fundamental spectrum. Measured and retrieved SPM spectra for $B_1 = 6.5$ (**e**) and $B_2 = 11$ (**f**).

4. Discussion and Conclusions

We demonstrated the experimental implementations of the simple non-interferometric method of pulse retrieval from fundamental and two SPM spectra using the novel algorithm of searching for a polynomial spectral phase. The algorithm was proposed and numerically investigated in [14]; here, we presented its first experimental verification on measured data. Namely, we reported the retrieval of (i) 670 fs pulses using a nonlinear silica-based fiber and (ii) 160 fs pulses using a chalcogenide (arsenic-sulfide-based) fiber. The obtained results are in a good agreement with the independent standard SHG-FROG measurements. Use of a chalcogenide fiber as a nonlinear element for the tested method is also demonstrated for the first time. Although, pulses were retrieved in the range of about 1.5 μm (not in the mid-IR range, as was numerically studied in [14]), the successful application of chalcogenide fibers allows us to propose their use as nonlinear Kerr elements for characterizing ultrashort pulses in a wider wavelength range corresponding to the transparency band of such fibers.

We worked in the dispersionless approximation, but the fiber dispersion should be taken into account for shorter pulses (when the relation $L_D >> L$ is not satisfied). Previously, we realized a Gerchberg–Saxton-like algorithm with allowance for the dispersion and demonstrated its experimental verification [10]. The novel algorithm of searching for a polynomial spectral phase considered here can be also modified in a similar way. $E_1(t)$ and $E_2(t)$ should be calculated from the nonlinear Schrödinger equation with the dispersion term [15] instead of Formulas (2) and (3) originated from Equation (1).

Author Contributions: Conceptualization, E.A.A.; methodology, E.A.A. and A.V.A.; software, E.A.A.; validation, E.A.A., A.A.S. and A.V.A.; formal analysis, A.A.S. and E.A.A.; investigation, E.A.A.; data curation, E.A.A.; writing—original draft preparation, E.A.A.; writing—review and editing, A.V.A.; resources, A.V.A.; supervision, E.A.A. All authors have read and agreed to the published version of the manuscript.

Funding: The work was supported by the Center of Excellence «Center of Photonics» funded by the Ministry of Science and Higher Education of the Russian Federation, Contract No. 075-15-2022-316.

Institutional Review Board Statement: Not applicable.

Informed Consent Statement: Not applicable.

Data Availability Statement: Data underlying the results presented in this article may be obtained from the authors upon reasonable request.

Conflicts of Interest: The authors declare no conflict of interest.

References

1. Trebino, R. *Frequency-Resolved Optical Gating: The Measurement of Ultrashort Laser Pulses*; Kluwer Academic Publishers: Boston, MA, USA, 2002.
2. Walmsley, I.A.; Dorrer, C. Characterization of Ultrashort Electromagnetic Pulses. *Adv. Opt. Photonics* **2009**, *1*, 308–437. [CrossRef]
3. Trebino, R.; Jafari, R.; Akturk, S.A.; Bowlan, P.; Guang, Z.; Zhu, P.; Escoto, E.; Steinmeyer, G. Highly Reliable Measurement of Ultrashort Laser Pulses. *J. Appl. Phys.* **2020**, *128*, 171103. [CrossRef]
4. Miranda, M.; Arnold, C.L.; Fordell, T.; Silva, F.; Alonso, B.; Weigand, R.; L'Huillier, A.; Crespo, H. Characterization of Broadband Few-Cycle Laser Pulses with the d-Scan Technique. *Opt. Express* **2012**, *20*, 18732–18743. [CrossRef]
5. Goda, K.; Jalali, B. Dispersive Fourier Transformation for Fast Continuous Single-Shot Measurements. *Nat. Photonics* **2013**, *7*, 102–112. [CrossRef]
6. Sugavanam, S.; Fabbri, S.; Le, S.T.; Lobach, I.; Kablukov, S.; Khorev, S.; Churkin, D. Real-Time High-Resolution Heterodyne-Based Measurements of Spectral Dynamics in Fibre Lasers. *Sci. Rep.* **2016**, *6*, 23152. [CrossRef] [PubMed]
7. Zahavy, T.; Dikopoltsev, A.; Moss, D.; Haham, G.I.; Cohen, O.; Mannor, S.; Segev, M. Deep Learning Reconstruction of Ultrashort Pulses. *Optica* **2018**, *5*, 666–673. [CrossRef]
8. Lapre, C.; Billet, C.; Meng, F.; Ryczkowski, P.; Sylvestre, T.; Finot, C.; Genty, G.; Dudley, J.M. Real-Time Characterization of Spectral Instabilities in a Mode-Locked Fibre Laser Exhibiting Soliton-Similariton Dynamics. *Sci. Rep.* **2019**, *9*, 13950. [CrossRef] [PubMed]
9. Anashkina, E.A.; Ginzburg, V.N.; Kochetkov, A.A.; Yakovlev, I.V.; Kim, A.V.; Khazanov, E.A. Single-Shot Laser Pulse Reconstruction Based on Self-Phase Modulated Spectra Measurements. *Sci. Rep.* **2016**, *6*, 33749. [CrossRef] [PubMed]
10. Anashkina, E.A.; Andrianov, A.V.; Koptev, M.Y.; Kim, A.V. Complete Field Characterization of Ultrashort Pulses in Fiber Photonics. *IEEE J. Sel. Top. Quantum Electron.* **2018**, *24*, 8700107. [CrossRef]
11. Baudin, K.; Audo, F.; Finot, C. Fiber-Based Measurement of Temporal Intensity and Phase Profiles of an Optical Telecommunication Pulse through Self-Phase Modulation. *Microw. Opt. Technol. Lett.* **2018**, *60*, 882–886. [CrossRef]
12. Anashkina, E.A.; Koptev, M.Y.; Andrianov, A.V.; Dorofeev, V.V.; Singh, S.; Leuchs, G.; Kim, A.V. Reconstruction of Optical Pulse Intensity and Phase Based on SPM Spectra Measurements in Microstructured Tellurite Fiber in Telecommunication Range. *J. Lightw. Technol.* **2019**, *37*, 4375–4381. [CrossRef]
13. Anashkina, E.A.; Andrianov, A.V.; Leuchs, G. Single-Shot Reconstruction of a Subpicosecond Pulse from a Fiber Laser System via Processing Strongly Self-Phase Modulated Spectra. *Results Phys.* **2020**, *16*, 102848. [CrossRef]
14. Sorokin, A.A.; Andrianov, A.V.; Anashkina, E.A. Numerical Study of Mid-IR Ultrashort Pulse Reconstruction Based on Processing of Spectra Converted in Chalcogenide Fibers with High Kerr Nonlinearity. *Fibers* **2022**, *10*, 81. [CrossRef]
15. Agrawal, G.P. *Nonlinear Fiber Optics*, 6th ed.; Elsevier: Amsterdam, The Netherlands, 2019.

16. Anashkina, E.A.; Andrianov, A.V.; Muravyev, S.V.; Kim, A.V. All-Fiber Design of Erbium-Doped Laser System for Tunable Two-Cycle Pulse Generation. *Opt. Express* **2011**, *19*, 20141–20150. [CrossRef] [PubMed]
17. Andrianov, A.V.; Koptev, M.Y.; Anashkina, E.A.; Muravyev, S.V.; Kim, A.V.; Lipatov, D.S.; Velmiskin, V.V.; Levchenko, A.E.; Bubnov, M.M.; Likhachev, M.E. Tapered Erbium-Doped Fibre Laser System Delivering 10 MW of Peak Power. *Quantum Electron.* **2019**, *49*, 1093–1099. [CrossRef]